Thin Solid Films 668 (2018) 9–13

Contents lists available at ScienceDirect

Thin Solid Films

journal homepage: www.elsevier.com/locate/tsf

Effect of the A1 to $L1_0$ transformation on the structure and magnetic properties of polycrystalline $Fe_{56}Pd_{44}$ alloy thin films produced by thermal evaporation technique

S. Bahamida[a,b], A. Fnidiki[b], M. Coïsson[c,*], G. Barrera[c], F. Celegato[c], E.S. Olivetti[c], P. Tiberto[c], A. Laggoun[a], M. Boudissa[d]

[a] Research unit UR-MPE, University of Boumerdes, 1 Avenue de l'Independance, 35000 Boumerdes, Algeria
[b] Groupe de Physique des Matériaux, Université et INSA de Rouen, UMR CNRS 6634 -Normandie Université, F-76801, Saint Etienne duRouvray, France
[c] INRIM, Nanoscience and Materials Division, strada delle Cacce 91, 10135 Torino (TO), Italy
[d] ENMC Laboratory, Department of Physics, Faculty of Sciences, University Ferhat Abbas, Setif 19000, Algeria

ARTICLE INFO

Keywords:
Iron-palladium alloy
Thin film structural transformation
Evaporation
X-ray diffraction
Conversion electron Mössbauer spectrometry
Magnetic properties

ABSTRACT

X-ray diffraction, conversion electron Mössbauer spectroscopy and superconducting quantum interference device magnetometer techniques have been used to characterize the evolution of the microstructure and of the magnetic properties of phase transformation from disordered FePd face-centred cubic (A1) phase, to an ordered phase $L1_0$ FePd of tetragonal structure. This study was carried out by isothermally annealing in vacuum at 550 °C, as a function of annealing time, a $Fe_{56}Pd_{44}$ thin film alloy deposited on silicon substrate.

The structural transformations are accompanied by a decrease of the (c/a) ratio and by an increase of the coercive field as a function of annealing time. After 10 min of annealing, the (c/a) ratio is equal to 0.945, which indicates that the disordered FePd phase is completely transformed into the ordered $L1_0$ FePd phase. By increasing annealing time, the microstructure of the alloy evolves, antiphase boundaries and twin boundaries develop. In contrast to the relationship most commonly described in the literature, that the highest coercivity corresponds to a two-phase ordered/disordered mixture, in ours studies the maximum value for coercivity corresponds to the fully ordered state. Furthermore, we propose that the high coercivity in these films is due to pinning centres of magnetic domain walls by antiphase boundaries and twin boundaries.

1. Introduction

High uniaxial magnetocrystalline anisotropy K_u in the range $2–6.6{\cdot}10^7$ erg/cm^3 has been found for alloys such Fe—Pd, Fe—Pt and Co—Pt [1]. These alloys are attractive for ultrahigh density magnetic recording and strong permanent magnet applications. The magnetic properties of these alloys are closely related to the microstructure of the tetragonal phase, which arises from the A1 → $L1_0$ transformation [2]. In the Fe—Pd, Fe—Pt and Co—Pt systems the ordered $L1_0$ phase is the stable phase at low temperatures and forms in conjunction with a first-order cubic (Al) to tetragonal ($L1_0$) transformation generally via a nucleation and growth process [3]. Hence, the microstructures that develop in ordered ferromagnetic alloys are tweed-like and polytwinned [2–4].

The tweed structure can develop during the A1 → $L1_0$ transformation, to relieve the lattice mismatch strain [2,4]. The polytwinned structure can develop after the atomic ordering transformation (A1 → $L1_0$). Because of this tetragonal lattice misfit of the tetragonal phase with the cubic phase matrix, a large amount of strain energy is induced. The formation of the polytwinned structure is due to the minimization of this atomic ordering strain energy [5].

Importantly, the tweed structure and the polytwinned structure are accompanied by the formation of structural defects, such as antiphase boundaries and twin boundaries. These defects play a role in determining the coercivity mechanism and the magnetization reversal [2–4]. Several studies have been focused on the coercivity mechanism (high coercivity) for the $L1_0$ ferromagnetic alloys. They have found that the increase of the coercivity is due to the pinning of the magnetic domains walls by the antiphase boundaries and the twin boundaries [2,3]. This has been deduced by the Lorentz microscopy imaging technique associated with the conventional transmission electron microscopy technique, which allows to visualize the magnetic domain

* Corresponding author.
E-mail address: m.coisson@inrim.it (M. Coïsson).

https://doi.org/10.1016/j.tsf.2018.10.013
Received 23 May 2018; Received in revised form 1 October 2018; Accepted 8 October 2018
Available online 09 October 2018
0040-6090/

structure and the microstructure respectively. These defects are characterised by a magnetic property, their hyperfine field, that can be measured by the Mössbauer spectrometry technique [6].

In this study, we report the results of our studies in a $Fe_{56}Pd_{44}$ thin film alloy, produced by thermal evaporation, which is a comparatively inexpensive technique; the film has been annealed at 550 °C as a function of time. We have focussed on the evolution of the structural and magnetic properties of phase transformation from disordered FePd face-centred cubic (A1) phase, to an ordered phase $L1_0$ FePd of tetragonal structure. To this aim, we have used different techniques: the X-ray diffraction to relate the crystallographic structure, the Mössbauer spectrometry for the microstructural transformations, and the superconducting quantum interference device magnetometry for the magnetic proprieties. The goal is to investigate how defects develop and how they affect the magnetic properties when transforming a disordered alloy into an ordered phase. We will show that an adequate development of defects can be exploited in improving the hard magnetic properties of the thin film.

2. Experimental procedure

A $Fe_{56}Pd_{44}$ thin film was grown on a silicon substrate by thermal evaporation. The alloy was prepared from elemental Fe and Pd powders of 99.99% purity. The mixed powder is deposited in a tungsten crucible placed in high vacuum chamber (base pressure 10^{-5} Pa). The operation pressure and applied average current were fixed to $7{\cdot}10^{-4}$ Pa and 124 A respectively. Chemical composition of the sample was determined by energy dispersive analysis by X-rays (EDX) with a relative error of 2% Pd. The thickness of the alloy films was measured by scanning electron microscopy (SEM): the sample was cut and placed in cross section under the electron beam, which was accelerated at 5 kV. The measured thicknesses is 80 nm and the average error in the thickness is around 4%. In order to promote phase transformations in the alloy, annealing treatments in vacuum (base pressure 10^{-5} Pa) at 550 °C for different annealing times were performed on selected specimens cut from the as-deposited sample. The alloy structure was studied using a glancing angle X-ray diffractometer (Pan'alytical X'pert PRO) with a CoK_α radiation source ($\lambda = 0.178897$ nm); the angle of incidence was of 1°.

Conversion Electron Mössbauer Spectrometry (CEMS) technique is used in order to analyse the first 100 nm in depth from the sample surface [7,8], at room temperature. CEMS experiments are performed at constant acceleration in reflection geometry using a ^{57}Co source diffused into a rhodium matrix (1.85 GBq). A He-CH_4 gas flow proportional counter is used to record the conversion (7.3 keV) and Auger (5.5 keV) electrons emitted after the resonant α-ray scattering by ^{57}Fe nuclei. The films were set perpendicular to the incident γ- beam. Isomer shifts (IS) at ^{57}Fe nuclei are given relative to α-Fe at 300 K.

The magnetic properties were measured at room temperature with a superconducting quantum interference device magnetometer (SQUID) at 300 K with an applied field parallel to the film surface (maximum field applied for the measurements 4.77 MA/m).

3. Results and discussion

X-ray diffraction patterns of the studied samples are shown in Fig. 1. The pattern related to the $Fe_{56}Pd_{44}$ thin film alloys before annealing is characterised by the fundamental peaks (111), (200), (220) and (311), which are associated to the single disordered FePd phase with face centred cubic (fcc) structure consistent with the literature [9]. We also deduced the lattice parameter a (3.814 ± 0.014) Å. This value is close to that of the FePd bulk alloy, which is equal to 3.80 Å [10].

Annealing at 550 °C for different times induces significant variations in the XRD patterns. The appearance of the super-lattices (110) and (201) and the splitting of the (200), (220) and (311) peaks in the X-ray diagrams of these films have been observed for all the annealed films. As the annealing time increases, the intensity of the super-lattice peaks

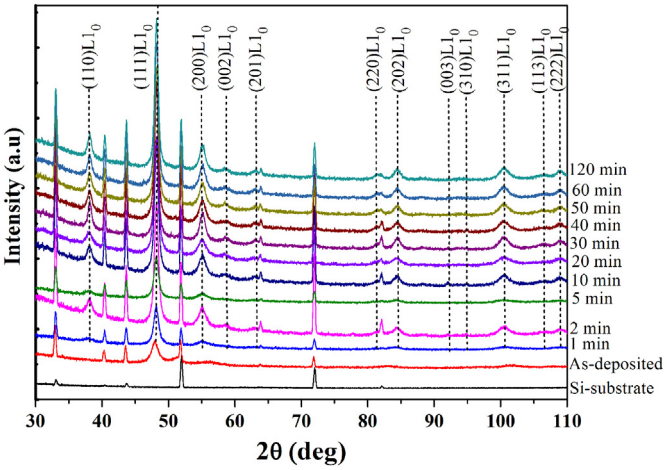

Fig. 1. X-ray diffraction patterns of as-deposited and annealed at 550 °C as a function annealing time for $Fe_{56}Pd_{44}$ thin film alloy.

increases indicating the increase in the degree of ordering in the $Fe_{56}Pd_{44}$ alloy. This variation is due to the transformation from the disordered face-centred-cubic (fcc) structure into the $L1_0$ ordered face-centred-tetragonal (fct) structure occurring during annealing [9]. This ordering transformation involves a decrease in size along the z-axis (perpendicular to the plane film) and an increase along x and y-axes, leading to tetragonality with the lattice parameter ratio (c/a) < 1.

Fig. 2 shows the lattice parameters a and c as well as the ratio (c/a) for the $L1_0$ FePd phase as a function of annealing time; these parameters are calculated with the Bragg equation, using both the (111) and (200) peaks. With increasing aging time, a increases from (3.814 ± 0.017) Å to (3.871 ± 0.017) Å, whereas c decreases from (3.814 ± 0.014) Å to (3.660 ± 0.014) Å. There is a large change in the lattice constants up to 10 min annealing, especially for c, after which the rate of change with aging time gets smaller. This is also reflected on the (c/a) ratio, which decreases from 1 to (0.945 ± 0.049) rapidly in the beginning with increasing time. This is a signature of the total transformation of the disordered FePd phase into the ordered $L1_0$ FePd phase.

The obtained ratio (c/a = 0.945) is slightly smaller than that reported for the bulk phase (~0.96) [10], but acceptably within the experimental uncertainty. Any internal strains possibly present in the material during deposition must have relaxed after annealing, and in any case would not affect the c/a ratio but only the peak widths. Anyway, these values perfectly match with those reported in literature for $L1_0$ FePd films grown by electro-deposition and subsequent thermal

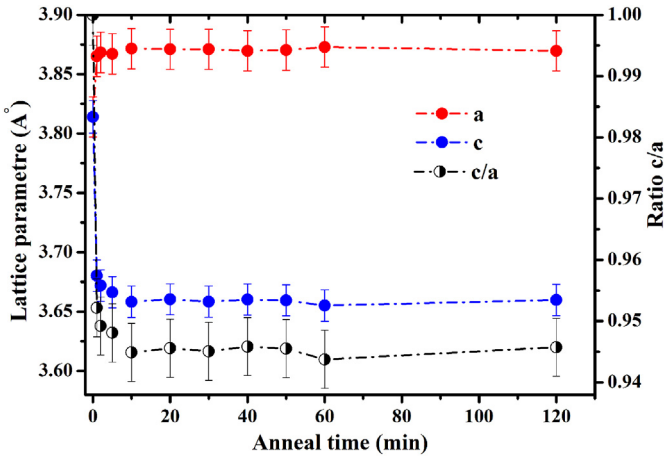

Fig. 2. Lattice parameters a, c and ratio (c/a) as a function of annealing time for $L1_0$ FePd phase.

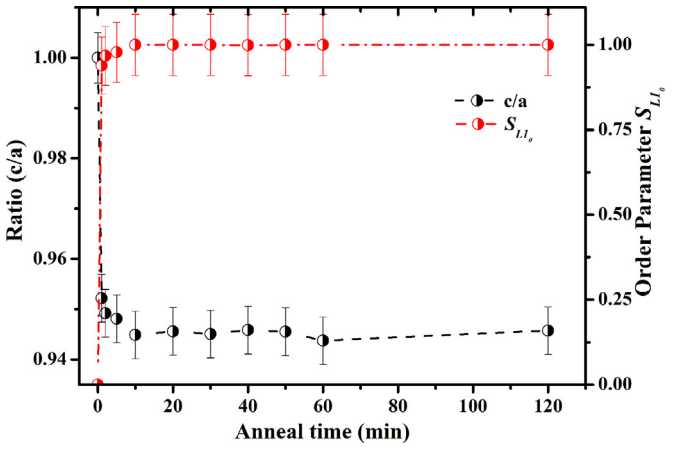

Fig. 3. c/a ratio (black symbols) and S_{L1_0}order parameter (red symbols) as a function of annealing time for $L1_0$ FePd phase. (For interpretation of the references to color in this figure legend, the reader is referred to the web version of this article.)

annealing onto polycrystalline titanium substrates, obtaining $a = 3.87$ Å and $c = 3.67$ Å [11]. For$Fe_{64}Pd_{36}$ thin film alloys grown on the silicon (100) substrate by thermal evaporation, the lattice parameters of the $L1_0$ FePd phase are $a = 3.85$ Å and $c = 3.67$ Å with the ratio (c/a) equal to 0.953 [12].

During the heat treatment, ordering in $Fe_{56}Pd_{44}$ alloy, characterizing the passage of the disordered phase FePd to ordered phase $L1_0$ FePd, takes place gradually with the annealing temperature at 550 °C as a function of the annealing time. Therefore, the S_{L10} order parameter of order phase is evaluated after each annealing time; S_{L10} is a function of the ratio (c/a) accordingly to references [13, 14], and can be written as follows: $S^2_{L10} = \left[\left(1 - {}^{c}/_{a}\right)/\left(1 - {}^{c}/_{a}\Big|_{s=1}\right)\right]$. Fig. 3 shows the evolution of the ratio c/a and of the order parameter S_{L10} of the ordered phase $L1_0$ FePd as a function of the annealing time. The figure clearly shows the opposite trends of the two curves. For all annealing times, the X-ray diffractograms reveal the presence of superstructure peak (110) indicating the presence of the $L1_0$ FePd phase. From this observation, it is clear that the phase transform in the $Fe_{56}Pd_{44}$ alloy is monophasic. After 1 min, we notice the rapid increase of the order parameter which reaches a value of 0.94, beyond which it becomes independent of the annealing time, within the experimental uncertainties.

In order to investigate in greater details the evolution of the $Fe_{56}Pd_{44}$ thin film alloys structure with thermal treatments, CEMS measurements have been performed, that are summarised in Fig. 4. Symbols represent the experimental data, whereas solid lines correspond to the fits. For each sample, the associated hyperfine magnetic field (HMF) contribution is also reported. For all samples, a clear ferromagnetic sextet can be observed, whose wide line width may be ascribed to a contribution of HMF caused by atomic distribution at near-neighbour sites of ^{57}Fe nuclei. The hyperfine parameters and their typical uncertainties obtained by the fits are summarised in Table 1.

The Mössbauer spectrum of the as-deposited $Fe_{56}Pd_{44}$ thin film has been fitted with the individual contribution detected by X-ray diffraction pattern analysis (Fig. 4a). This contribution is associated with the disordered $Fe_{50}Pd_{50}$ phase face-centred-cubic (fcc) structure. From the fitting parameters, reported in Table 1, the mean hyperfine field value is (25.99 ± 0.24) MA/m and the mean isomer shift value is (0.1680 ± 0.005) mm/s. The obtained value of the hyperfine field is closer to the value reported by Longworth [15] for disordered $Fe_{50}Pd_{50}$ (25.47 MA/m), but it is lower than the value reported by Gehanno et al. [16] which is equal to 27.30 MA/m. The angle between the magnetization direction and the normal to the film plane was estimated to 75°, indicating that the easy axes of magnetization lie, locally, on average close to the sample plane. Hence, the sample is characterised by

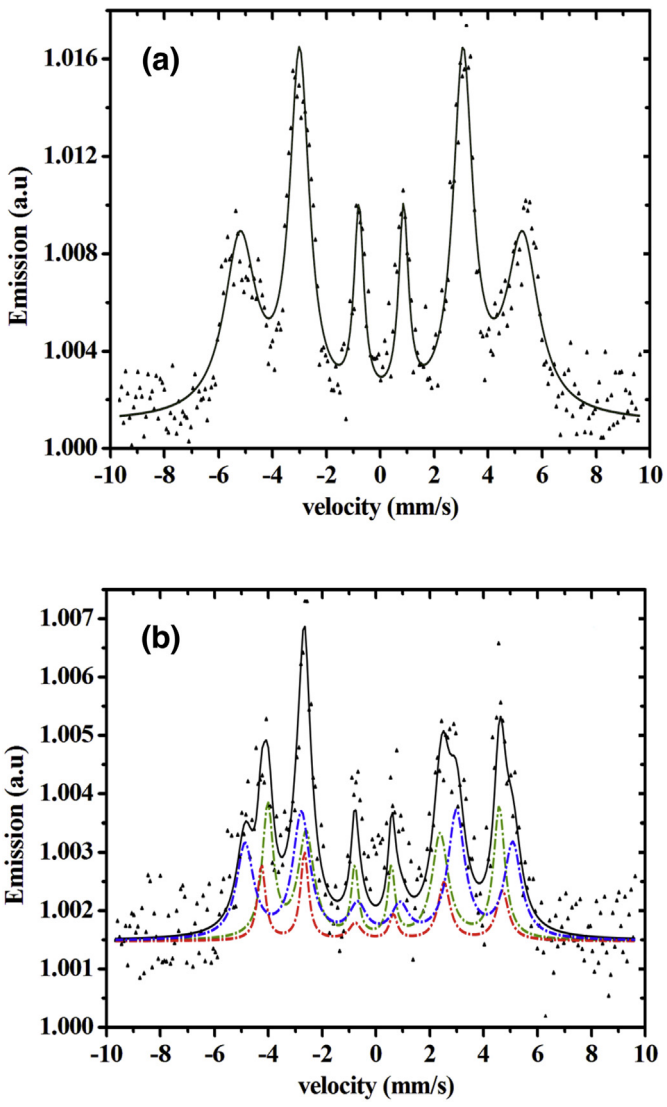

Fig. 4. Mössbauer spectrum of the $Fe_{56}Pd_{44}$ thin film alloy (symbols: experimental data, lines: fits) (a) as-prepared and (b) annealed at 550 °C for 60 min (ordered $L1_0$ FePd phase (green), twin boundaries (red), antiphase boundaries (blue), the $Fe_{56}Pd_{44}$ thin film alloys (black)). (For interpretation of the references to colour in this figure legend, the reader is referred to the web version of this article.)

dominant shape anisotropy.

For the $Fe_{56}Pd_{44}$ thin film alloys annealed at 550 °C, the Mössbauer spectrum shows some asymmetry and the onset of intermediate lines; Fig. 4b reports as an example the data relative to the sample annealed for 60 min. Three contributions were assumed. The first contribution accounting for 38.72% of the iron atomic fraction belongs to the fct $L1_0$ FePd phase. The mean hyperfine field and the quadrupole splitting are (21.33 ± 0.24) MA/m and (0.389 ± 0.005) mm/s respectively. The obtained value for the hyperfine field is closer to the value reported for ordered $Fe_{50}Pd_{50}$ by Longworth [15] and by Tsurin et al. [6] which are 21.06 MA/m and 21.32 MA/m respectively, whereas Gehanno et al. [16] have found a hyperfine field of 21.97 MA/m. The second and the third contributions can be associated with the small intermediate lines, which are attributed to the larger hyperfine filed values of 22.21 MA/m and 24.68 MA/m respectively. Hence, these contributions can be associated to structural defects [6,16,17].

Tsurin et al. [6] have analyzed the Mössbauer spectra of bulk $L1_0$ FePd polycrystalline samples with three contributions. The first one corresponding to large ordered regions with a hyperfine field and a

Table 1
Mössbauer parameters of as-prepared and annealed at 550 °C samples: ⟨H_{hf}⟩ average hyperfine magnetic field, ⟨θ⟩ average angle between the normal to the sample plane and the hyperfine magnetic field, ⟨QS⟩ quadrupolar splitting, ⟨DI⟩ isomer shift.

$Fe_{56}Pd_{44}$	Atomic fraction %	(⟨H_{hf}⟩ ± 0.24) (MA/m)	(⟨QS⟩ ± 0.005) (mm/s)	(⟨DI⟩ ± 0.005) (mm/s)	(⟨θ⟩ ± 5) (°)	Contribution
As-deposited	100	25.99	0.000	0.168	75	Disordered fcc FePd phase
Annealing 550 °C	38.72	21.33	0.389	0.112	75	Ordered $L1_0$ FePd phase
	15.86	22.21	0.289	0.090	75	Twin boundaries
	45.42	24.68	0.000	0.132	90	Antiphase boundaries (APB)

quadrupole splitting of 21.06 MA/m and 0.3825 mm/s respectively. The second one was associated to twin-oriented domains, with a hyperfine field of 22.49 MA/m and a quadrupole splitting of 0.289 mm/s. The last one, with a hyperfine field of 24.68 MA/m, was attributed to antiphase boundaries. In the case of Gehanno et al. [16,17], their study focused on the magnetic properties of the FePd thin films deposited on the MgO substrate; by the analysis of the Mössbauer spectroscopy they found a broadening in the hyperfine field distribution which is due to the presence of structural defects (twin boundaries and antiphase boundaries). Indeed, structural defects such as twin boundaries and antiphase boundaries have been shown to generate perturbed regions with larger hyperfine field values with respect to the ordered phase, and whose values are pretty much coincident with those measured in our annealed samples.

These structural defects turn out to play a significant role in the magnetic properties (e.g. coercive field) of the alloy. It is worth noting that the combined atomic fraction of the twin boundaries and of the antiphase boundaries amounts to approximately 61% of the total atoms. From the XRD data, the average crystallite size of the sample annealed for 60 min is of approximately 16 nm (8 nm radius), which means that the surface-to-volume ratio is rather large. As antiphase and twin boundaries are a result of the interfacing of adjacent crystallites, their relative significance, as evidenced by the Mössbauer analysis, appears justified by the small crystallite size. Also for the annealed samples, the angle at which the average magnetisation vector lies with respect to the normal to the substrate is 75° for the $L1_0$ phase and the twin-oriented domains, and 90° for antiphase boundaries, indicating that even in presence of a strong magnetocrystalline anisotropy (due to the $L1_0$ phase), the easy axes are predominantly oriented close to the sample plane.

The hysteresis loops of the studied samples have therefore been measured at room temperature by applying in-plane magnetic fields, and the results are shown in Fig. 5. The as-deposited film is characterised by the softest magnetic behaviour, having a coercive field of 400 A/m and a remanence to saturation ratio (Mr/Ms) of 0.38. This result is in agreement with both X-ray and Mössbauer results, which indicates the presence of the disordered face-centred-cubic FePd phase.

For the films annealed at 550 °C for different time, the loops significantly change shape. The coercivity increases with increasing annealing time, indicating that the sample becomes magnetically harder. At 10 min annealing time, the coercivity is equal to 106.7 kA/m. This change in the coecitivity is associated to the total transformation of the disordered FePd phase into ordered $L1_0$ FePd phase in the alloy in agreement with X-ray results. After long annealing time (60 min), the coercivity reaches the value of 157.1 kA/m. By comparing the in-plane and out-of-plane hysteresis loops of the sample annealed for 60 min, it is evident that the anisotropy axes of the tetragonal crystallites are not aligned along any preferential direction in space. The high remanence to saturation ratio for the in-plane loop suggests that rotation processes are not significant for this sample, in agreement with Mössbauer data that indicate an average distribution of the anisotropy axes of the crystallites along directions tilted by 75° with respect to the normal to the film plane. Moreover, according to the results of the Mössbauer spectrometry the microstructure of the alloy has further changed, with the formation of antiphase boundaries and twin boundaries. These results suggest that the high coercivity is induced not only by the order-disorder transformation but also by the structural defects.

In fact,generally speaking, defects in the $L1_0$ ordered ferromagnetic alloys, such as antiphase boundaries and twin boundaries as well as phase boundaries (ordered/disordered), can form pinning centres that impede the movement of magnetic domain walls, leading to high coercivity [2–4,18]. Several works were realized to understand the origin of these structural defects and the mechanisms of high coercivity in the ordered ferromagnetic alloys. Ritau et al. [17] have examined the order-disorder transformation in CoPt and FePt thin films annealed at 700 °C. They have suggested that the high coercivity mechanism in these thin films is due to the magnetic domain wall pinning at the phase boundaries (ordered/disordered) and at the antiphase boundaries. Wang et al. [2] have used different techniques, i.e. the Lorentz microscopy imaging to study the magnetic domain structure and the conventional transmission electron microscopy to visualize the microstructure in the $Fe_{55}Pd_{45}$ alloy, as well as the VSM to measure the magnetic properties at different stages of atomic ordering. At low annealing temperature, they have found that the antiphase boundaries are

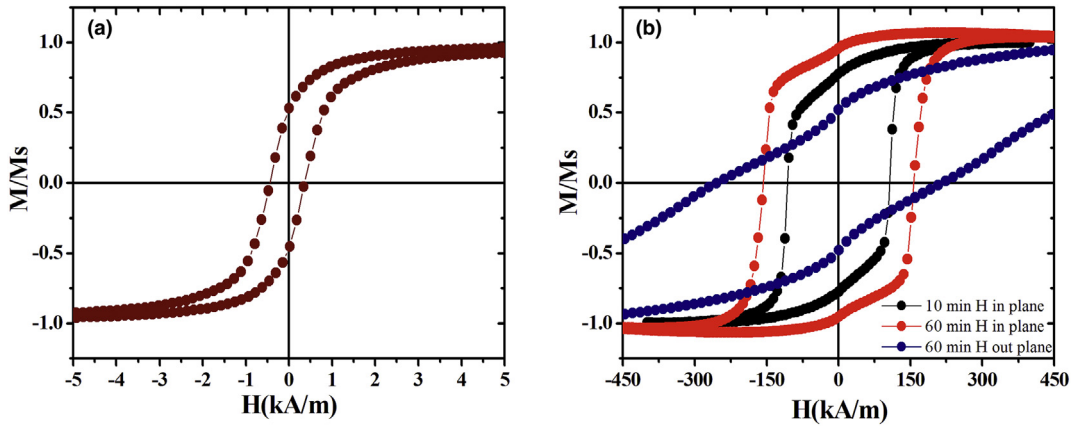

Fig. 5. Hysteresis loops for $Fe_{56}Pd_{44}$ thin film: (a) as-deposited; (b) annealed at 550 °C for 10 min (black curve), 60 min in-plane (red curve) and out-of-plane (blue curve). (For interpretation of the references to colour in this figure legend, the reader is referred to the web version of this article.)

formed in the tweed structure, while the twin boundaries are formed in the polytwinned structure, at higher annealing temperature. Also, they have deduced that the mechanism of high coercivity is due to the wall pinning at the antiphase boundaries and the twin boundaries.

In the present study, magnetic measurements reveal that a hard magnetic behaviour is achieved already after 10 min annealing, when XRD reveal a complete transformation of the disordered soft phase into the $L1_0$ one. However, coercivity still increases when annealing is continued, as the development of the tetragonal phase induces the formation of antiphase boundaries and twin boundaries that are all detected by Mössbauer spectroscopy. Their presence results in a further increase of the coercivity.

4. Conclusion

The $A1 \rightarrow L1_0$ phase transformation has been studied in the $Fe_{56}Pd_{44}$ alloy system in thin films form submitted to thermal treatments at 550 °C in vacuum as a function of annealing time. Combined structural (CEMS and XRD) and magnetic (SQUID) measurements revealed that the phase transformation is complete after just 10 min annealing, but the subsequent evolution of the $L1_0$ phase, with the development of twinned domains, twin boundaries and antiphase boundaries, is quite effective in contributing to the magnetic properties and in increasing the value of the coercive field. This study has therefore proved that in order to optimise the hard magnetic properties of the $Fe_{56}Pd_{44}$ thin films, the microstructure evolution must be carefully followed in order to exploit not only the development of the $L1_0$ phase, but also of its structural defects, that in proper conditions act favourably to the increase of coercivity.

References

[1] N.I. Vlasova, G.S. Kandaurova, N.N. Shchegoleva, Effect of the polytwinned microstructure parameters on magnetic domain structure and hysteresis properties of the CoPt-type alloys, J. Magn. Magn. Mater. 222 (2000) 138.

[2] L. Wang, D.E. Laughlin, Y. Wang, A.G. Khachaturyan, Magnetic domain structure of Fe-55 at.% Pd alloy at different stages of atomic ordering, J. Appl. Phys. 93 (2003) 7984.

[3] T. Klemmer, D. Hoydick, H. Okumura, B. Zhang, W.A. Soffa, Magnetic hardening and coercivity mechanisms in $L1_0$ ordered FePd ferromagnets, Scr. Metall. Mater. 33 (1995) 1793.

[4] B. Zhang, W.A. Soffa, Magnetic domains and coercivity in polytwinned ferromagnets, Phys. Status Solidi 131 (1992) 707.

[5] L. Wang, Z. Fan, D.E. Laughlin, Trace analysis for magnetic domain images of $L1_0$ polytwinned structures, Scripta Mater. 47 (2002) 781.

[6] V.A. Tsurin, A.E. Ermakov, Y.G. Lebedev, B.N. Filippov, A Mössbauer study of the structural characteristics of equiatomic FePd and FePt alloys, Phys. Status Solidi (a) 33 (1976) 325.

[7] C. Lemoine, A. Fnidiki, F. Danoix, M. Hédin, J. Teillet, Mössbauer and atom probe studies on the ferrite decomposition in duplex stainess steels caused by the quenching rate, J. Phys. 11 (1999) 1105.

[8] F. Richomme, A. Fnidiki, J. Teillet, M. Toulemonde, Tb/Fe amorphous multilayers: transformations under ions irradiation, Nucl. Instrum. Methods B 107 (1996) 374.

[9] A. Chbihi, Etude de l'effet d'une déformation plastique préalable sur les transformations de phases dans les alliages modèles: CuCr et FePd, Université de Rouen, 2011 (PhD Thesis, In French).

[10] W. B. Pearson, Handbook of Lattice Spacings and Structures of Metals, 2018 Pergamon Press, ed. G.V. Raynor, (revised edition 1958, ISBN 9781483226613).

[11] F.M. Takata, G. Pattanaik, W.A. Soffa, P.T.A. Sumodjo, G. Zangari, Synthesis of $L1_0$ Fe-Pd films by electrodeposition and thermal annealing, Electrochem. Commun. 10 (2008) 568.

[12] S. Bahamida, A. Fnidiki, M. Coïsson, A. Laggoun, G. Barrera, F. Celegato, P. Tiberto, Mixed exchange-coupled soft α-($Fe_{80}Fe_{20}$) and hard $L1_0$ FePd phases in $Fe_{64}Pd_{36}$ thin films studied by first order reversal curves, Mater. Sci. Eng. B 226 (2017) 47.

[13] B.W. Roberts, X-ray measurement of order in CuAu, Acta Meter. 2 (1954) 597.

[14] J.A. Christodoulides, P. Farber, M. Dannl, H. Okumura, G.C. Hadjipanayis, V. Skumryev, A. Simopoulos, D. Weller, Magnetic, structural and microstructural properties of FePt/M (M = C, BN) granular films, IEEE Trans. Magn. 37 (2001) 1292.

[15] G. Longworth, Temperature dependence of the ^{57}Fe hfs in the ordered alloys $FePd_3$ and FePd near the Curie temperature, Phys. Rev. 172 (1968) 572.

[16] V. Gehanno, P. Auric, A. Marty, B. Gilles, Structural and magnetic properties of epitaxial $Fe_{0.5}Pd_{0.5}$ thin films studied by Mössbauer spectroscopy, J. Magn. Magn. Mater. 188 (1998) 310.

[17] V. Gehanno, Anisotropie magnétique perpendiculaire des couches minces épitaxiées D'Alliage ordonnes FePd, University Joseph-Fourier-Grenoble I, France, 1997 (PhD thesis, In French).

[18] R.A. Ristau, K. Barmak, L.H. Lewis, K.R. Coffey, J.K. Howard, On the relationship of high coercivity and $L1_0$ ordered phase in CoPt and FePt thin films, J. Appl. Phys. 86 (1999) 4527.